# Intrinsic and Environmental Effects in the Structure and Magnetic Properties of Glycine Radical in Aqueous Solution

**Nadia Rega, Maurizio Cossi, and Vincenzo Barone***

*Contribution from the Dipartimento di Chimica, Università di Napoli "Federico II", via Mezzocannone 4, I-80134 Napoli, Italy*

*Received June 5, 1997. Revised Manuscript Received October 17, 1997*[⊗]

**Abstract:** The electron spin resonance (ESR) spectrum of the radicals derived from glycine in aqueous solution has not been reproduced satisfactorily until now, even by refined quantum mechanical approaches. Here we will show that a recently developed computational tool provides, instead, results in remarkable agreement with experiment. The computational protocol is based on density functional calculations, on the simulation of the solvent with a continuous dielectric description, and on averaging over the most important vibrational motions. Both the direct polarization and the geometry relaxation induced by the solvent on the glycine radical are analyzed, and their effect on the ESR spectra is evaluated. The present procedure is able to separate the various intrinsic and environmental contributions and to provide useful insight to the structural study of large flexible radicals in solution.

## 1. Introduction

Chemical interest for organic free radicals is still growing since these species are key intermediates in a number of reactions of industrial as well as biological significance. In particular, the effect of radiation on aqueous solution of biological materials leads to the formation of OH radicals, which, in turn, attack biomolecules leading to radical intermediates issuing from addition or elimination reactions. While a full characterization of these intermediates would provide significant mechanistic information, this task is not simple from an experimental point of view since spectroscopic techniques usually can only be employed and the relationships between spectroscopic parameters and structural features is quite indirect. Futhermore, the measured quantities often result from the superposition of different contributions which are very difficult, when not impossible, to separate. In such circumstances, quantum mechanical computations can provide an invaluable support to experiment since they are able to selectively switch a number of interactions on and off, evaluating the effect of different contributions. The only problem is that the computational models must be at the same time reliable and rapid enough to allow the study of sufficiently large systems. In recent years we have shown[1−3] that hybrid density functional/Hartree−Fock (HF) methods are quite promising in this connection when coupled to proper treatments of averaging effects issuing from large amplitude vibrations. More recently, we have extended this computational protocol to condensed phases,[3,4] adding to the above features the self-consistent effect of a polarizable continuum mimicking the solvent. Since the first results of this new protocol were very promising, we have decided to study an important and quite difficult problem, namely the nature of the species issuing from the homolytic breaking of the C−H bond of glycine in aqueous solution at different pH.

From an experimental point of view, it has been concluded that, contrary to the parent molecule, this radical prefers a neutral structure (i.e., $NH_2-\dot{C}H-COOH$ in place of $NH_3^+-\dot{C}H-COO^-$) even in aqueous solution[5,6] and that the cationic form ($NH_3^+-\dot{C}H-COOH$) is not dominant even at pH = 1.[6] Furthermore, the electron spin resonance (ESR) spectra show some unexpected features like an anomalously low isotropic hyperfine coupling constant (hcc) of about 12 G for the hydrogen directly bonded to the radical center ($H^\alpha$) and a complete equivalence between the hydrogens of the amine group.[6] On the other hand, the ESR spectrum of the zwitterionic form in the solid state shows a more usual hcc of 26.8 G for $H^\alpha$.[7] Previous quantum mechanical studies were only partially successful since the characteristics of the zwitterionic species were well reproduced,[8] but the isotropic hyperfine coupling constants of the neutral form were not in full agreement with experiment, and the situation was not improved by the description of the solvent by a simple quantum-Onsager model.[9]

From a more general point of view, a satisfactory description of this system shows the potential impact of quantum-mechanical techniques in the field of biomolecules. The more so as the whole computational approach is well standardized and is or will be shortly available to other researchers in the field through standard packages.

## 2. Computational Methods

The calculations were performed with a modified version of the GAUSSIAN94 package,[10] at the unrestricted Kohn−Sham (UKS) level using the so called B3LYP hybrid functional, which combines Hartree−Fock and Becke[11] exchange with the Lee−Yang−Parr[12] correlation functionals. Geometries were optimized using the 6-31G** basis set;

[⊗] Abstract published in *Advance ACS Abstracts,* December 15, 1997.

(1) Barone, V. *Theor. Chim. Acta* **1995**, *91*, 113.
(2) Barone, V. *J. Phys. Chem.* **1995**, *99*, 11659.
(3) Barone, V. *Chem. Phys. Lett.* **1996**, *262* , 201.
(4) Rega, N.; Cossi, M.; Barone, V. *J. Chem. Phys.* **1996**, *105*, 11060.
(5) Paul, von H.; Fischer, H. *Helv. Chim. Acta* **1971** , *54*, 485.
(6) Neta, P.; Fessenden, R. W. *J. Phys. Chem.* **1971**, *75*, 738.
(7) Ghosh, D. K.; Wiffen, D. H. *J. Chem. Soc.* **1960**, 1869.
(8) Barone, V.; Adamo, C.; Grand, A.; Subra, R. *Chem. Phys. Lett.* **1995**, *242*, 35.
(9) Barone, V.; Adamo, C.; Grand, A.; Jolibois, F.; Brunel, Y.; Subra, R. *J. Am. Chem. Soc.* **1995**, *117*, 12618.
(10) Frisch, M. J.; Trucks, G. W.; Schlegel, H. B.; Gill P. M. W.; Johnson B. G.; Robb, M. A.; Cheeseman J. R.; Keith, T.; Petersson G. A.; Montgomery, J. A.; Raghavachari, K.; Al-Laham, M. A.; Zakrzewski, V. G.; Ortiz, J. V.; Foresman, J. B.; Peng, C. Y.; Ayala, P. Y.; Chen, W.; Wong, M. W.; Andres, J. L.; Replogle, E. S.; Gomperts, R.; Martin, R. L.; Fox, D. J.; Binkley, J. S.; Defrees, D. J.; Baker, J.; Stewart, J. P.; Head-Gordon, M.; Gonzalez, C.; Pople, J. A. GAUSSIAN94, *Revision D.4*, Gaussian, Inc.: Pittsburgh, PA, 1995.
(11) Becke, A. D. *Phys. Rev. B* **1988**, *38*, 3098.
(12) Lee, C.; Yang, W.; Parr, R. G. *Phys. Rev. B* **1988**, *37*, 785.

S0002-7863(97)01838-6 CCC: $14.00 

energies and spectroscopic constants were computed with the so called EPR-2 basis set,[4,13] developed by our group for this kind of applications. In all the SCF calculations, tight convergence thresholds were adopted (i.e., $10^{-6}$ au for energies and $10^{-8}$ for root mean square density changes): more modest convergence criteria do not provide reliable values for the observables we are interested in, which critically depend on the wave function quality.

Hyperfine coupling constants are obtained from the spin Hamiltonian[14]

$$\hat{H}_{\text{spin}} = -g\beta_e S_z B_z - g_N \beta_N I_z B_z + \mathbf{SAI} \qquad (1)$$

where $\beta_e$ and $\beta_N$ are the electron and nuclear magneton, respectively; **S** is the magnetic moment of unpaired electrons and **I** that of magnetic nuclei; $g_N$ is the nuclear magnetogyric ratio, and $g$ is the free electron magnetogiric ratio. The isotropic components of the tensor **A** (i.e., the isotropic coupling constants (hcc) measured by ESR spectroscopists), are related to the spin densities at the nuclei:

$$a(N) = \frac{8\pi}{3}\beta_e g_N \beta_N \sum_{\mu\nu} \mathbf{P}^{\alpha-\beta}_{\mu\nu} \langle \phi_\mu | \delta(\vec{r}_N) | \phi_\nu \rangle \qquad (2)$$

where $\mathbf{P}^{\alpha-\beta}$ is the difference between the density matrices of electrons $\alpha$ and $\beta$. Throughout this article the hcc values are expressed in Gauss and can be converted into megahertz by multiplying them by 2.8025.

The solvent effect has been reproduced by the polarizable continuum model (PCM),[15] recently implemented in the GAUSSIAN94 package by our group.[16] In the PCM framework the solvent is represented as an infinite polarizable medium characterized by its dielectric constant (78.4 in the case of water at 25 °C): the solute molecules are embedded in cavities formed by the envelope of atomic spheres, following the well-known GEPOL procedure,[17] and the solvent polarization is described by means of apparent charges distributed on the cavity surface.

The PCM allows us to determine the molecular free energy in solution, which is usually partitioned into four contributions:

$$G = G_{\text{cav}} + G_{\text{dis}} + G_{\text{rep}} + G_{\text{el}} \qquad (3)$$

The first three terms are related to the work needed to build the cavity in the solvent (cavitation free energy) and to the solute−solvent dispersion and repulsion interactions: they are calculated with the classical approaches described in refs 18 and 19. The last term in eq 3, referred to as the electrostatic solute−solvent interaction, is usually the most important, especially for polar solutes in solvents with high dielectric constants, and it is calculated ab initio: the present implementation is able to find the polarization charges and the solute wave function polarized by the solvent with a single self-consistent field calculation. The electrostatic interaction affects both the free energy and the electronic properties, such as the hcc's, of the solute. The calculation in the presence of the solvent can be performed at the HF, density functional (DF), and post-HF (many body perturbation theory, configuration interaction, and coupled clusters) levels.[16] The PCM procedure can also optimize the solute geometry taking into account the solvent effect at the HF and DF levels.[20,21] In this article, Pauling's atomic radii ($r$(C) = $r$(N) = 1.5 Å, $r$(O) = 1.4 Å, $r$(H) =1.0 Å when the hydrogen is bound to N or O, $r$(H) = 1.2 Å when it is bound to C) have been used to build the solute cavities; the various terms in eq 3 require different definitions of the cavities, as explained (e.g., in ref 16) in particular, when calculating electrostatic energies the above radii are scaled by the factor 1.2.

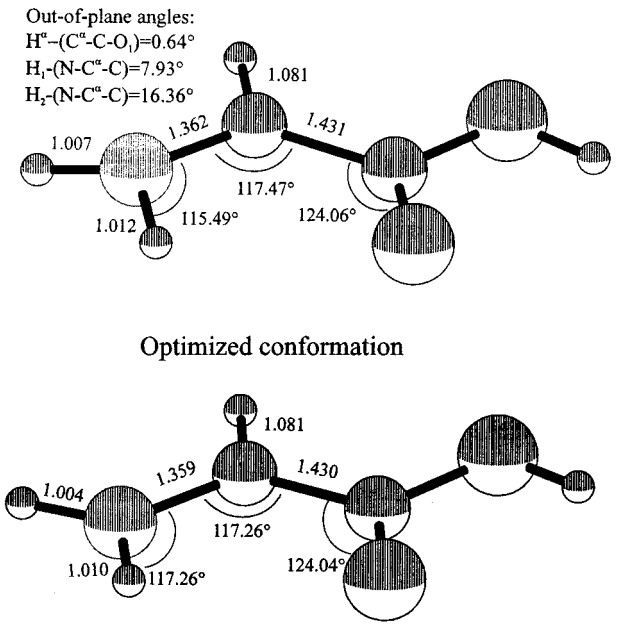


**Figure 1.** Main geometrical parameters (angstroms and degrees) for the glycine radical optimized in vacuo at the B3LYP/6-31G** level.

The PCM results have been compared to the values obtained with another well-known solvation model implemented in the GAUSSIAN94 package, namely, the single-center multipole expansion (SCME) model by Rivail and co-workers.[22,23] Also, this approach describes the solvent as a polarizable dielectric, but the solute electrostatic potential is expanded in a multipole series and the solvent polarization is found in terms of a reaction field related to the terms of this series: the SCME can use molecular cavities similar to the PCM ones or simpler cavities (i.e., spheres and ellipsoids).

Vibrational averaging can be very important for an accurate hcc computation, since the spin density at some nuclei can change significantly even for motions of not too large amplitude. In the present work, the results have been averaged over the most important vibrational motions using the DiNa program,[24] developed by our group, following the procedure illustrated in refs 4 and 13.

## 3. Results and Discussion

In Figure 1 we report the geometry of the glycine radical optimized in vacuo at the B3LYP/6-31G** level, along with the planar geometry obtained with a constrained optimization. Though the former structure corresponds to the real minimum in the potential energy hypersurface, the latter is more representative due to large amplitude vibrational motions that are discussed below.

The direct solvent effect on the calculated hcc values was evaluated at the B3LYP/EPR-2 level, with the results listed in Table 1. In this context, "direct" effect indicates the effect of the solvent induced polarization on the solute wave function, keeping the geometry optimized in vacuo fixed. The indirect effects, related to the solvent induced geometry relaxation, are analyzed below.

(13) Barone, V. In *Recent Advances in Density Functional Methods*; Chong, D. P., Ed.; World Scientific: Singapore, 1995; Part 1.
(14) Weltner, W., Jr. *Magnetic Atoms and Molecules*; van Nostrand: New York, 1983.
(15) Miertuš, S.; Scrocco, E.; Tomasi, J. *Chem. Phys.* **1981**, *55*, 117.
(16) Cossi, M.; Barone, V.; Cammi, R.; Tomasi, J. *Chem. Phys. Lett.* **1996**, *255*, 327.
(17) Pascual-Ahuir, J. L.; Silla, E.; Tunon, I. *J. Comput. Chem.* **1994**, *15*, 1127.
(18) (a) Floris, F. M.; Tomasi, J. *J. Comput. Chem.* **1989**, *10*, 616. (b) Floris, F. M.; Tomasi, J.; Pascual-Ahuir, J. L. *J. Comput. Chem.* **1991**, *12*, 784. (c) Cossi, M.; Mennucci, B.; Cammi, R. *J. Comput. Chem.* **1996**, *17*, 717.
(19) Pierotti, R. *Chem. Rev.* **1976**, *76* , 717.
(20) Cossi, M.; Tomasi, J.; Cammi, R. *Int. J. Quantum Chem., Quantum Chem. Symp.* **1995**, *29*, 625.
(21) Barone, V.; Cossi, M.; Tomasi, J. *J. Comput. Chem.* In press.
(22) Rivail, J. L.; Rinaldi, D. In *Computational Chemistry: Review of Current Trends;* Lesckzynski, J., Ed.; World Scientific: Singapore, 1995.
(23) Dillet, V.; Rinaldi, D.; Bertran, J.; Rivail, J. L. *J. Chem. Phys.* **1996**, *104*, 9437.
(24) (a) Minichino, C.; Barone, V. *J. Chem. Phys.* **1994**, *100*, 3717. (b) Barone, V; Minichino, C. *THEOCHEM* **1995**, *330*, 365.

**Table 1.** Dipole Moment (Debye) and hcc's (Gauss) Calculated at B3LYP/EPR-2 Level for the Glycine Radical at the Geometries Optimized in Vacuo

| | fully optimized geometry | | planar geometry | | experimental values in aqueous solution[a] |
|---|---|---|---|---|---|
| | in vacuo | in solution | in vacuo | in solution | |
| $\|\mu\|$ | 2.69 | 3.63 | 2.80 | 3.77 | |
| $a$(N) | 6.06 | 6.40 | 3.39 | 4.05 | 6.38 |
| $a(C^{\alpha})$ | 12.28 | 9.23 | 11.23 | 8.00 | |
| $a$(C) | −8.99 | −6.75 | −8.69 | −6.33 | |
| $a(O_1)$ | −3.79 | −3.68 | −3.77 | −3.70 | |
| $a(O_2)$ | −0.10 | −0.72 | −0.14 | −0.78 | |
| $a(H^{\alpha})$ | −14.71 | −12.91 | −14.40 | −12.73 | 11.77 |
| $a(H_1)$ | −5.31 | −5.89 | −8.12 | −8.90 | 5.59 |
| $a(H_2)$ | −2.04 | −2.89 | −8.51 | −9.38 | 5.59 |
| $a(H_0)$ | −1.56 | −1.71 | −1.59 | −1.75 | |

[a] Absolute values, from ref 6.

**Table 2.** Dipole Moment (Debye) and hcc's (Gauss) Calculated at B3LYP/EPR-2 Level for the Glycine Radical in the Planar Conformation Optimized in Vacuo, with SCRF Solvent Model (Spherical Cavity with Radius 3.34 Å) at Different Multipole Orders

| | | SCRF | | | | | | |
|---|---|---|---|---|---|---|---|---|
| | in vacuo | $l = 1$ | $l = 2$ | $l = 3$ | $l = 4$ | $l = 5$ | $l = 6$ | $l = 7$ |
| $\|\mu\|$ | 2.80 | 3.50 | 3.69 | 3.73 | 3.88 | 3.93 | 4.01 | 4.07 |
| $a$(N) | 3.39 | 3.65 | 4.08 | 4.08 | 4.16 | 4.14 | 4.12 | 4.11 |
| $a(C^{\alpha})$ | 11.23 | 9.79 | 8.60 | 8.50 | 8.13 | 8.10 | 8.00 | 7.94 |
| $a$(C) | −8.69 | −7.67 | −7.01 | −6.95 | −6.73 | −6.71 | −6.64 | −6.61 |
| $a(O_1)$ | −3.77 | −3.91 | −3.79 | −3.81 | −3.79 | −3.78 | −3.78 | −3.79 |
| $a(O_2)$ | −0.14 | −0.24 | −0.50 | −0.51 | −0.56 | −0.56 | −0.57 | −0.57 |
| $a(H^{\alpha})$ | −14.40 | −13.63 | −12.94 | −12.94 | −12.72 | −12.69 | −12.64 | −12.61 |
| $a(H_1)$ | −8.12 | −8.40 | −8.98 | −8.96 | −9.11 | −9.10 | −9.09 | −9.09 |
| $a(H_2)$ | −8.51 | −8.85 | −9.45 | −9.43 | −9.57 | −9.55 | −9.50 | −9.46 |
| $a(H_0)$ | −1.59 | −1.61 | −1.66 | −1.66 | −1.65 | −1.65 | −1.65 | −1.65 |

It is noteworthy that the calculated hcc for the $H^{\alpha}$, the most significant from the experimental point of view due to its anomalously low value, is markedly improved by the consideration of the solvent polarization: notice that the $a(H^{\alpha})$ values obtained by good quality post-HF calculations on the isolated radical[9] were even farther from the experiment than the present B3LYP results. In the past,[9] the poor agreement between the measured value and the best available calculations on the isolated radical raised many doubts about the structure of the glycine radical in solution: it appears that the solvent effect must be taken into account to compare experimental and theoretical results properly.

Also, the calculated value of the nitrogen coupling constant is closer to the experimental data when the solvent effect is considered. On the other hand, the values for the aminic hydrogens remain quite dissimilar in the equilibrium structure, whereas they become nearly equivalent in the planar geometry, thus suggesting that indirect solvent effects and vibrational averaging can be important to improve the agreement with the experiment.

To investigate how the computed hcc's depend on the solvent model, we repeated the calculations for the planar configuration with the SCME procedure: in Table 2 we report the SCME results obtained by truncating the multipole expansion at different levels ($l$ ), using a simple spherical cavity of radius 3.34 Å, having the same volume as the PCM cavity.

The SCME results for the spherical cavity become comparable to the PCM ones at high orders of the multipole expansion only: this is also true when more elaborated cavities, namely, ellipsoidal and GEPOL, are used. Here we don't report the SCME results obtained with a GEPOL cavity, since in this case the solvent effect on the calculated hcc's is very low: in fact this SCME implementation uses atomic radii different from those adopted in PCM, and the resulting GEPOL cavities are quite larger. Notice that the PCM cavities, based on the Pauling set of atomic radii, have been selected by reproducing the solvation energies of a number of neutral and ionic compounds, as explained in ref 16. Anyway, we performed a PCM calculation with the same radii as in SCME, obtaining hcc's values in good agreement with the SCME ones for $l \geq 4$ : the computational times requested for this SCME and the PCM calculations are practically the same.

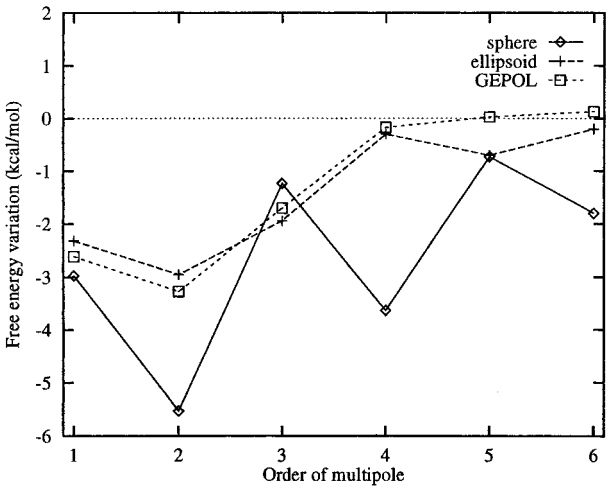


**Figure 2.** Free energy variations with respect to the isolated radical calculated with the SCME solvent model at different multipole orders with spherical, ellipsoidal, and GEPOL cavities.

In a previous study,[9] use of the SCME approach truncated at the level of a dipole in a spherical cavity led to a very modest environmental effect on the isotropic hcc's of the glycine radical: the present results show that it is necessary to go well further in the multipolar expansion to obtain reliable values. Furthermore, as shown in Figure 2, the multipole expansion is not fully converged even at high levels, particularly for the spherical cavity.

In Table 3 we report the glycine radical geometrical parameters optimized in solution at the B3LYP/6−31G** level,

**Table 3.** Geometrical Parameters (angstroms and degrees) for the Glycine Radical Optimized at the B3LYP/6-31G** Level in Vacuo and in Solution: Both the Real Minimum and the Planar Conformation Are Reported

| | fully optimized geometry | | planar conformation | |
|---|---|---|---|---|
| | in vacuo | PCM | in vacuo | PCM |
| bond lengths | | | | |
| $C^a-N$ | 1.362 | 1.356 | 1.359 | 1.354 |
| $C^a-C$ | 1.431 | 1.427 | 1.430 | 1.427 |
| $C-O_1$ | 1.232 | 1.239 | 1.233 | 1.239 |
| $C-O_2$ | 1.366 | 1.360 | 1.367 | 1.360 |
| $C^a-H^\alpha$ | 1.081 | 1.083 | 1.081 | 1.083 |
| $O-H$ | 0.970 | 0.971 | 0.970 | 0.971 |
| $N-H_1$ | 1.012 | 1.013 | 1.010 | 1.011 |
| $N-H_2$ | 1.007 | 1.010 | 1.004 | 1.009 |
| $O_1-H_1$ | 2.371 | 2.426 | 2.381 | 2.401 |
| bond angles | | | | |
| $N-C^\alpha-C$ | 117.47 | 118.40 | 117.26 | 118.35 |
| $C^\alpha-C-O_1$ | 124.06 | 123.94 | 124.04 | 123.95 |
| $C^\alpha-C-O_2$ | 113.53 | 113.50 | 113.57 | 113.55 |
| $C-O-H$ | 105.10 | 106.76 | 105.02 | 106.69 |
| $H^\alpha-C^\alpha-C$ | 122.92 | 122.64 | 123.10 | 122.70 |
| $H_1-N-C^\alpha$ | 115.49 | 117.56 | 117.26 | 117.40 |
| $H_2-N-C^\alpha$ | 120.53 | 120.90 | 122.60 | 121.70 |
| out-of-plane angles | | | | |
| $H^\alpha-(C^\alpha-C-O_1)$ | 0.64 | 0.55 | 0.0 | 0.0 |
| $H_1-(N-C^\alpha-C_1)$ | 7.93 | 7.88 | 0.0 | 0.0 |
| $H_2-(N-C^\alpha-C)$ | 16.36 | 10.81 | 0.0 | 0.0 |

**Table 4.** Glycine Radical Dipole Moment (Debye) and hcc's (Gauss) in Solution Calculated by PCM at the B3LYP/EPR-2 Level: Equilibrium and Planar Conformations Optimized at the B3LYP/6-31G** Level in Vacuo and in Solution

| | equilibrium conformation | | planar conformation | | |
|---|---|---|---|---|---|
| | geometry optimized in vacuo | geometry optimized in solution | geometry optimized in vacuo | geometry optimized in solution | exptl (absolute values) |
| $\|\mu\|$ | 3.63 | 3.79 | 3.77 | 3.78 | |
| $a(N)$ | 6.40 | 5.49 | 4.05 | 4.04 | 6.38 |
| $a(C^\alpha)$ | 9.23 | 8.38 | 8.00 | 7.70 | |
| $a(C)$ | −6.75 | −6.58 | −6.33 | −6.29 | |
| $a(O_1)$ | −3.68 | −3.81 | −3.70 | −3.82 | |
| $a(O_2)$ | −0.72 | −0.77 | −0.78 | −0.80 | |
| $a(H^\alpha)$ | −12.91 | −12.85 | −12.73 | −12.56 | 11.77 |
| $a(H_1)$ | −5.89 | −6.71 | −8.90 | −8.91 | 5.59 |
| $a(H_2)$ | −2.89 | −6.05 | −9.38 | −9.35 | 5.59 |
| $a(H_0)$ | −1.71 | −1.80 | −1.75 | −1.82 | |

compared to the vacuum values both for the real minimum and for the planar structure.

In both the cases, the presence of the solvent shortens the C−N bond, whereas the C═O bond is sligthly longer, corresponding to a greater weight of the ionic resonance structures in polar media; moreover, the intramolecular hydrogen bond is markedly reduced in the solvent. The most significant result is that in solution the equilibrium structure is closer to planarity, since the out-of-plane angles of the aminic hydrogens and of the $H^\alpha$ are reduced: as observed in many cases, the structures with a higher degree of delocalization are favored by the solvent, since a greater charge separation increases the electrostatic solute−solvent interactions.

The effect of the solvent induced geometry relaxation on the hcc's is illustrated in Table 4, where we report the values calculated in solution with and without geometry reoptimization. The most important changes regard the aminic hydrogens in the equilibrium conformation: as the geometry optimized by PCM is more planar, the aminic hydrogens hcc's are much more similar to each other.

A comparison of Tables 1 and 4 shows that the direct solvent effects are more pronounced for $H^\alpha$, though the agreement with the experiment is further enhanced by considering the geometry relaxation too, whereas the indirect effects are more important for the aminic group.

**Table 5.** Glycine Radical hcc's (Gauss) Averaged over the Hydrogen Inversion Motion at 0 K and at 298 K

| | in vacuo | | in solution | | exptl (absolute values) |
|---|---|---|---|---|---|
| | 0 K | 298 K | 0 K | 298 K | |
| $a(N)$ | 5.25 | 5.81 | 5.39 | 5.67 | 6.38 |
| $a(C^\alpha)$ | 12.00 | 12.23 | 8.35 | 8.49 | |
| $a(H^\alpha)$ | −14.64 | −14.72 | −12.84 | −12.91 | 11.77 |
| $a(H_1)$ | −6.18 | −5.59 | −6.84 | −6.40 | 5.59 |
| $a(H_2)$ | −3.90 | −2.42 | −6.20 | −5.52 | 5.59 |

It is well-known that large amplitude vibrational motions, in particular hindered rotations and inversions involving the radical centers, may affect the ESR parameters significantly. For example, the calculated hcc for the carbon atom in the methyl radical is increased by about 30% when the out-of-plane motions of hydrogens are taken into account.[4] In the present case internal rotations are strongly hindered,[9] so we considered the inversion of the $H^\alpha$ and of the aminic hydrogens with respect to the molecular (N−C−C) plane only, for which the planar structure illustrated in Figure 1 and in Table 3 is the transition state. Since the energy difference between the pyramidal minimum conformation and the transition state is very low (0.12 kcal/mol in vacuo and 0.04 kcal/mol in solution), we simplified the treatment by considering a single motion involving all the three hydrogens, defined as the linear synchronous path (LSP) joining the minimum and the saddle point. The linear synchronous coordinate (LSC) is defined as the arc length along this path in mass weighted cartesian coordinates, taking into account the proper orientation of successive structures. The hcc's were calculated at the B3LYP/EPR-2 level both in vacuo and in solution for a number of structures along this path, obtaining the energy profiles shown in Figure 3a together with the first vibrational wave functions; in Figure 3b the dependence of $H^\alpha$ and $H_2$ hcc's on the LSC are illustrated. The hcc's were then averaged over the LSC with the DiNa procedure: in Table 5 we summarize the results at 0 K (i.e., averaged on the vibrational ground state only) and at 298 K, considering the first ten vibrational wave functions.

It is noteworthy that the energy profile in solution is narrower than in vacuo, consistently with the enhanced planarity induced by the polar medium. The calculated value of the $H^\alpha$ hcc is affected by the vibrational averaging slightly and at the same extent in vacuo and in solution, confirming that the solvent effect on this parameter is eminently due to direct polarization. On the other hand, the aminic hydrogens hcc's are sensibly affected by the out-of-plane motion: their vibrationally averaged values are closer to the experimental ones, and their equivalence is markedly enhanced, and both these effects are more pronounced in solution. Unlike the previous theoretical treatments, the B3LYP-PCM-DiNa approach proves capable to reproduce this challenging experimental parameter, too.

Considering the solvent effect by the PCM model substantially improves the agreement with the experiment for all the isotropic hcc's, in particular for the $H^\alpha$ hcc, which is the most interesting due to its anomalous observed value. A point of interest is whether the remaining discrepancy between the calculated and the experimental values could be eliminated by taking into account some specific water−glycine interactions that cannot be reproduced by a continuous model. It has already been verified that the spin transfer between this free radical and the solvent is very limited,[9] so that the effect of specific interactions should be rather to enhance the glycine polarization through strong H-bonds with the molecules of the first solvation shell.

**Table 6.** Hcc's (Gauss) Calculated at the B3LYP/EPR-2 Level for the Glycine Radical[a] Differently Solvated by Explicit Water Molecules and by PCM (see Figure 4 for Molecule Labeling)

| | Glycine + water 1 | Glycine + water 2 | Glycine + water 3 | Glycine + water 4 | Glycine + 4 $H_2O$ | Glycine + 4$H_2O$ + PCM | exptl (absolute values) |
|---|---|---|---|---|---|---|---|
| $a$(N) | 3.50 | 3.85 | 3.45 | 3.65 | 4.19 | 4.27 | 6.38 |
| $a$($C^{\alpha}$) | 10.52 | 8.99 | 10.18 | 10.02 | 6.17 | 5.69 | |
| $a$(C) | −7.78 | −6.89 | −8.21 | −8.03 | −4.78 | −4.49 | |
| $a$($O_1$) | −3.47 | −3.77 | −4.14 | −3.79 | −3.72 | −3.65 | |
| $a$($O_2$) | −0.79 | −0.66 | −0.02 | −0.22 | −1.35 | −1.45 | |
| $a$($H^{\alpha}$) | −14.13 | −13.20 | −13.92 | −13.72 | −11.81 | −11.57 | 11.77 |
| $a$($H_1$) | −8.23 | −8.63 | −8.14 | −8.47 | −8.94 | −9.07 | 5.59 |
| $a$($H_2$) | −8.65 | −9.11 | −8.56 | −8.82 | −9.42 | −9.53 | 5.59 |

[a] In the planar conformation optimized in vacuo.

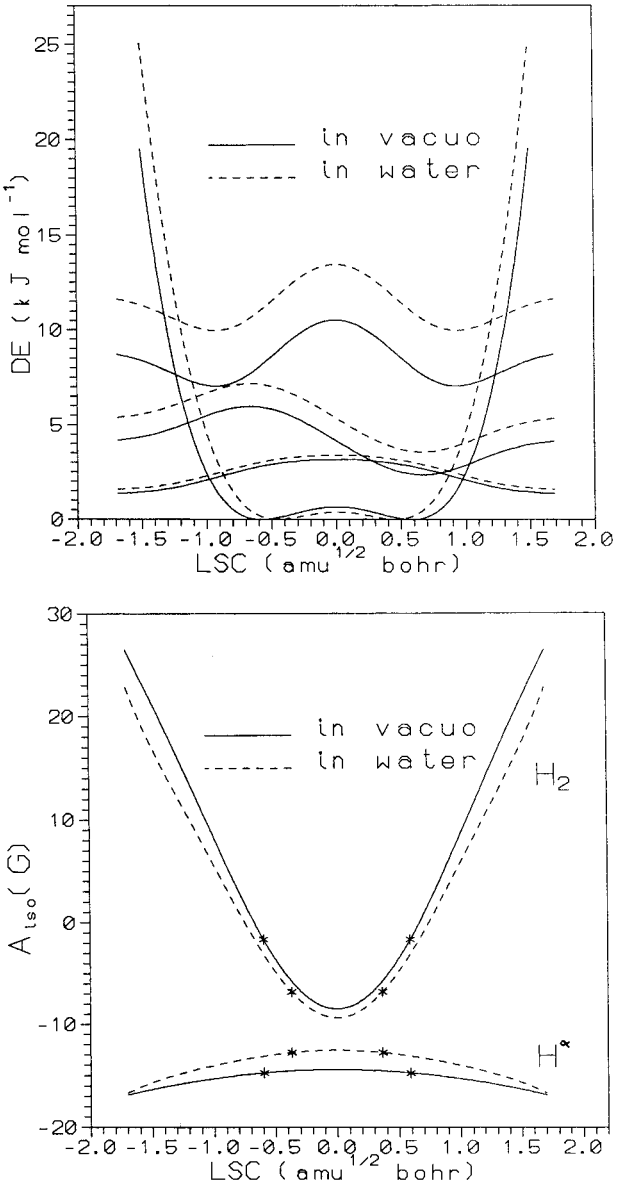


**Figure 3.** (a) Energy profiles in vacuo and in solution along the linear synchronous coordinate (LSC), corresponding to the inversion motion of $H^{\alpha}$ and of amidic hydrogens, and first vibrational eigenstates. (b) Values of $H^{\alpha}$ and $H_2$ hcc's along the LSC in vacuo and in solution.

To investigate this point we examined the glycine + 4 water cluster shown in Figure 4.

The number and the positions of the water molecules were determined by molecular dynamics simulations performed by the AMBER package,[25] with rigid water geometries and keeping the glycine in the planar conformation optimized in vacuo at the B3LYP/6-31G** level (see Table 3). The intermolecular parameters of each glycine−water couple were then optimized at the B3LYP/6-31G** level, and the results were assembled to prepare the system in Figure 4. The glycine ESR parameters were calculated at the B3LYP/EPRII level for each glycine−water couple, for the glycine + 4 $H_2O$ system and for the glycine + 4 $H_2O$ surrounded by the continuous solvent, with the results shown in Table 6.

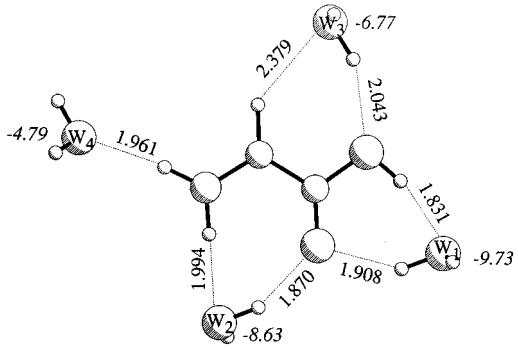


**Figure 4.** Glycine radical−water cluster: the intermolecular distances (in angstrom) and the binding energies (in kcal/mol) of each glycine−water pair are reported.

The calculations performed on the glycine + 4 $H_2O$ system closely reproduce the experimental $H^{\alpha}$ hcc: from Table 6 one can see that the water molecules have different effects on the various solute atoms, but the contribution of any solvent molecule cannot be neglected. Furthermore the effect of the bulk of the solvent, introduced by the surrounding continuous dielectric, although relatively small, cannot be neglected in quantitative work. Our most accurate result for the different hcc's is obtained adding to the values obtained at this level (Table 6, column 6) the contribution due to geometry relaxation (Table 4, column 4 minus column 3) and the contribution due to vibrational averaging (Table 5, column 4 minus Table 4, column 4). This leads to $a$(N) = 5.89 G; $a$($H^{\alpha}$) = −11.75 G; $a$($H_1$) = −6.57 G, and $a$($H_2$) = −5.67 G. All of these values are in fair agreement with the experiment.

A number of interesting conclusions can be drawn from these findings. The major part of the solvent effect on the glycine radical ESR parameters can be ascribed to the first solvation shell, and it is almost exclusively due to the polarization of the glycine wave function induced by the H-bonds with the solvent. The PCM model, though based on a simple and unstructured description of the solvent, is able to reproduce the effect of the first solvation shell on the wave function up to 70% (compare for example the solvent shift on $a$($H^{\alpha}$) due to PCM in the fourth column of Table 1 to that due to the first solvation shell in the

(25) Cornell, W. D.; Cieplak, P.; Bayly, C. I.; Gould, I. R.: Merz, K. M., Jr.; Ferguson, D. M.; Sellmeyer, D. C.; Fox, T.; Caldwell, J. W.; Kollman, P. A. *J. Am. Chem. Soc.* **1995**, *117*, 5179.

fifth column of Table 6), even when H-bonds are particularly important. Needless to say, the PCM calculations on the simple glycine radical are by far faster and easier than the calculations on the glycine−water clusters: in particular, the PCM geometry optimizations are nearly as efficient as those on the isolated radical.

## 4. Conclusions

We have presented a number of results concerning the calculation of ESR parameters for a prototypical free radical in aqueous solution. The solvent influence on the calculated hcc's revealed itself very important, and only computational procedures taking it into account are able to reproduce the experimental findings. Comparing the PCM continuous description of the solvent to explicit water−glycine clusters, we found that the PCM description can account for a large part of the total solvent effect on these subtle electronic properties.

Both the direct (polarization) and the indirect (geometry relaxation) solvent effects have to be considered to obtain reliable values of the ESR parameters for all the solute magnetic nuclei. The PCM procedure, as implemented in the GAUSSIAN94 package by our group, can efficiently describe both the effects at the density functional level, then it is particularly suited for this kind of application.

Some of the calculated ESR parameters are definitely improved by the vibrational averaging that can be easily obtained with the DiNa program coupled to the B3LYP-PCM procedure.

The same B3LYP-PCM-DiNa approach is being applied to other glycine radicals in aqueous solution, in particular to the radical anion, with the aim to reproduce the ESR spectra of this species over the whole pH range, and to investigate the structure of the free radicals produced in aqueous solution by hydrogen abstraction on aminoacidic residues. Furthermore, work is in progress to examine the electronic stabilization factors of some of these radicals and the influence of polar solvents on them.

**Acknowledgment.** We thank the Consiglio Nazionale delle Ricerche (CNR) for financial support to this research, and Professor J. L. Rivail for use of his SCME computer code.

**Supporting Information Available:** Tabulation of energies for the glycine radical at optimized geometries in vacuo and in solution (2 pages). This material is contained in libraries on microfiche, immediately follows this article in the microfilm version of the journal, and can be ordered from the ACS; see any current masthead page for ordering information.

JA971838Y